On the Higher Order Statistics of the Channel Capacity in Dispersed Spectrum Cognitive Radio Systems Over Generalized Fading Channels

Theodoros A. Tsiftsis, *Senior Member, IEEE,*
Fotis Foukalas, *Member, IEEE,*
George K. Karagiannidis, *Fellow, IEEE*, and
Tamer Khattab, *Member, IEEE*

Abstract—This work is devoted to the study of dispersed spectrum cognitive radio (CR) systems over independent and nonidentically distributed (i.n.i.d.) generalized fading channels. More specifically, this is performed in terms of the high-order statistics (HOS) of the channel capacity over $\eta-\mu$ fading channels. A generic analytic expression is derived for the corresponding nth statistical moment, which is subsequently employed for deducing exact closed-form expressions for the first four moments. Using these expressions, important statistical metrics, such as the amount of dispersion, amount of fading, skewness, and kurtosis, are derived in closed form and can be efficiently used in providing insights on the performance of dispersed CR systems. The obtained numerical results reveal interesting outcomes that could be useful for the channel selection, either for sharing or aggregation in heterogeneous networks, which is the core structure of future wireless communication systems.

Index Terms—Amount of dispersion, channel capacity, cognitive radio (CR), dispersed spectrum, high-order statistics (HOS).

I. INTRODUCTION

Cognitive radio (CR) is an emerging technology for the next generation of wireless communication systems, i.e., fifth generation (5G). CR can be efficiently implemented in heterogeneous networks (HetNets), wherein channels can be allocated from heterogeneous bands (i.e., nonadjacent bands) and their sharing or aggregation feature among several basestations and multiple users. These new cognitive-wise technologies deal with the dispersed nature of the heterogeneous spectrum bands. Thus, a *dispersed spectrum CR* over generalized fading channels can be assumed to study the performance of the next-generation wireless communication systems with CR capabilities (see [1] and the references therein).

Ergodic capacity, which is one of the most important performance metrics of wireless communication systems, has been extensively studied in the technical literature (see [2] and references therein).

Furthermore, higher order statistics (HOS) is a useful tool for calibrating the maximum dispersion in the channel capacity [3]. Considering that this dispersion is heavily affected by the heterogeneity that inherently exists in contemporary wireless communication networks, HOS can effectively lead to reliable communication designs. It is notable that the HOS of the channel capacity can provide critical information on the dispersion of capacity around a signal-to-noise ratio (SNR) value, and thus, insightful gains can be extracted for the transmission throughput reliability [3], [4]. The latter is very important in a new feature of 3GPP LTE-Advanced communication systems, called *carrier aggregation*, where multiple component carriers aggregated at the receiver side of a user equipment (UE) to get a wider bandwidth and, hence, increased data rate [5].

Prior works on the HOS of the capacity over generalized fading channels have been focused on the diversity receivers. In particular, Yilmaz and Alouini studied in [3] the HOS of the channel capacity for a receiver equipped with a maximal ratio combiner (MRC) over correlated generalized fading channels, where the HOS expressions were given in integral form. In [6], Sagias *et al.* studied the HOS of the capacity for several diversity receivers over independent and nonidentically distributed (i.n.i.d.) Nakagami-m fading channels and also proposed a new performance metric, called *fading figure* ($\mathcal{FF}$), which, similarly with the *amount of fading* ($\mathcal{AoF}$), is based on the variance of the capacity.

The first published work with performance analysis of ad hoc dispersed spectrum over Nakagami-m fading channels was presented in [1]. In this important paper, Qaraqe *et al.* studied the average symbol error probability of dispersed spectrum CR systems, for both ucorrelated/correlated fading environment. Moreover, in [1], the effective transport capacity of ad hoc dispersed spectrum CR networks in 3-D node distribution was investigated. Former works in this topic focused mostly on time delay estimation issues for localization and positioning applications [7]. To the best of our knowledge, the performance of dispersed spectrum CR systems has not been studied, considering the HOS of the channel capacity over generalized fading environment.

The main contribution of this paper is based on the analysis of HOS of the channel capacity. The study of HOS has attracted a lot of attention in wireless communications; however, most contributions are devoted to the analysis of the level crossing rate and average fade durations. On the contrary, the HOS of the capacity has been addressed in very few published works. Thus, the proposed contribution is meaningful, since it addresses the HOS of the channel capacity of dispersed spectrum CR systems over generalized fading channels. The derived results are novel and also are given in closed form for general fading channels, as opposed to previously published works. Specifically, in this paper, a dispersed spectrum CR system with generalized fading channels is considered, and the expressions for the HOS of the channel capacity are presented in closed form. The $\eta-\mu$ fading channel model is assumed for the dispersed spectrum CR, as a generalized fading model, which incorporates many special cases such as the Nakagami-q, Nakagami-m, Rayleigh, and one-sided Gaussian distributions. Useful statistical metrics, such as $\mathcal{FF}$, *amount of dispersion* ($\mathcal{AoD}$), *skewness* ($\mathcal{S}$), and *kurtosis* ($\mathcal{K}$), are analytically presented. Having defined the channel capacity of our model, we obtain the HOS expressions in closed form, which are useful in analyzing statistical metrics such as $\mathcal{AoD}$ [3], [4]. In addition to $\mathcal{AoD}$, which measures the maximum dispersion of the channel capacity in CR systems, we derive, in closed form, $\mathcal{FF}$, $\mathcal{S}$, and $\mathcal{K}$, highlighting further the behavior of the dispersed spectrum CR. All the aforementioned performance metrics can be efficiently used for

the best channel selection in heterogeneous wireless networks with spectrum sharing and/or aggregation capabilities.

The remainder of this paper is organized as follows: Section II describes the considered system and channel model. Section III is devoted to the derivation of the HOS of the channel capacity over $\eta-\mu$ fading channels for the dispersed spectrum CR. The respective numerical results and analysis are provided in Section IV, while concluding remarks are finally given in Section V.

II. SYSTEM AND CHANNEL MODEL

We consider a dispersed spectrum CR, which is similar to the ones studied in [1], [7], and [8]. Secondary users (SUs) perform spectrum sensing to identify which bands are available and, thus, to exploit the benefits of frequency diversity by combining the instantaneous SNRs γ_is, from each diversity band. By assuming L available frequency diversity bands, the end-to-end SNR at the output of each SU's receiver is given by

$$\gamma_{\text{end}} = \sum_{i=1}^{L} \gamma_i. \tag{1}$$

Each frequency diversity channel is assumed to be slow and frequency nonselective and subject to i.n.i.d. $\eta-\mu$ fading. The $\eta-\mu$ distribution is a generalized fading model that has been shown to provide accurate characterization of *small-scale* fading in non-line-of-sight (NLOS) communications. It was presented for the first time by the pioneering work of Yacoub in [9] and shown that $\eta-\mu$ is a flexible fading model, including, as special cases, the Nakagami-q (Hoyt), Nakagami-m, Rayleigh, and one-sided Gaussian distributions. The $\eta-\mu$ fading model is expressed by two parameters η and μ and is valid for two different formats, namely, *Format-1* and *Format-2*. In the former, the η parameter represents the ratio of the powers between the multipath waves in the in-phase and quadrature components, whereas in the latter, it represents the correlation coefficient between the scattered wave in-phase and quadrature components of each cluster of multipath. Furthermore, the μ parameter denotes, in both formats, the inverse of the normalized variance and is related to the respective number of multipath clusters [9]–[11].

The probability density function (PDF) of the instantaneous SNR in $\eta-\mu$ fading channels is given by [12, eq. (3)]

$$f_{\gamma_{\eta-\mu}}(\gamma) = \frac{2\sqrt{\pi}\mu^{\mu+\frac{1}{2}}h^{\mu}}{\Gamma(\mu)H^{\mu-\frac{1}{2}}} \frac{\gamma^{\mu-\frac{1}{2}}}{\overline{\gamma}^{\mu+\frac{1}{2}}} e^{-2\mu h\frac{\gamma}{\overline{\gamma}}} I_{\mu-\frac{1}{2}}\left(\frac{2\mu H\gamma}{\overline{\gamma}}\right) \tag{2}$$

where γ and $\overline{\gamma}$ denotes the instantaneous and average SNR, respectively; $\Gamma(x)$ is the Gamma function; and $I_n(x)$ is the modified Bessel function of the first kind with argument x and order n. Parameters h and H are defined as follows:

$$h_{\text{F}-1} = \frac{(2+\eta^{-1}+\eta)}{4} \tag{3}$$

$$H_{\text{F}-1} = \frac{(\eta^{-1}-\eta)}{4} \tag{4}$$

with $0 < \eta < \infty$ for *Format-1* and

$$h_{\text{F}-2} = \frac{1}{(1-\eta^2)} \tag{5}$$

$$H_{\text{F}-2} = \frac{\eta}{(1-\eta^2)} \tag{6}$$

with $-1 < \eta < 1$ for *Format-2*.

Furthermore

$$\mu = \frac{[\mathbb{E}(R^2)]^2}{2\text{Var}(R^2)}\left[1+\frac{H}{h}\right] \tag{7}$$

for both formats with $\mathbb{E}(.)$ and $\text{Var}(.)$ denoting statistical expectation and variance of the envelope R, respectively [9].

With the aid of the finite series representation for integer values of μ [13, eq. (8.467)], $I_n(x)$ in (2) can be equivalently rewritten as [11], [14]–[17]

$$I_{\mu-\frac{1}{2}}\left(\frac{2\mu H\gamma}{\overline{\gamma}}\right) = \sum_{l=0}^{\mu-1} \frac{(-1)^l\Gamma(\mu+l)\overline{\gamma}^{l+\frac{1}{2}}e^{\frac{2\mu H\gamma}{\overline{\gamma}}}}{l!\sqrt{\pi}\Gamma(\mu-l)(4\mu H\gamma)^{l+\frac{1}{2}}}$$
$$+ \sum_{l=0}^{\mu-1} \frac{(-1)^\mu\Gamma(\mu+l)\overline{\gamma}^{l+\frac{1}{2}}e^{-\frac{2\mu H\gamma}{\overline{\gamma}}}}{l!\sqrt{\pi}\Gamma(\mu-l)(4\mu H\gamma)^{l+\frac{1}{2}}}. \tag{8}$$

By substituting (8) into (2) and carrying out basic algebraic manipulations, it follows that

$$f_{\gamma_{\eta-\mu}}(\gamma) = \sum_{k=0}^{\mu-1} \frac{(\mu)_k\mu^{\mu-k}h^\mu\gamma^{\mu-k-1}}{k!H^{\mu+k}\Gamma(\mu-k)2^{2k}\overline{\gamma}^{\mu-k}}$$
$$\times \left[(-1)^k e^{-2\mu(h-H)\frac{\gamma}{\overline{\gamma}}} + (-1)^\mu e^{-2\mu(h+H)\frac{\gamma}{\overline{\gamma}}}\right] \tag{9}$$

which is valid for $\mu \in \mathbb{N}$.

III. HIGH-ORDER STATISTICS OF THE CHANNEL CAPACITY

The average spectral efficiency (i.e., the average ergodic capacity normalized to the available bandwidth B) can be expressed as [3], [6]

$$\mathbb{E}(S^n) = \mathbb{E}\left[\log_2^n(1+\gamma_{\text{end}})\right] \tag{10}$$

where $n \in \mathbb{N}$ denotes the order of the statistics, which is particularly useful in quantifying the maximum dispersion of the channel capacity [2]. By substituting (1) into (10), the following L-fold integral is readily deduced, i.e.,

$$\mathbb{E}(S^n) = \int_0^\infty \int_0^\infty \cdots \int_0^\infty \log_2^n\left(1+\sum_{i=1}^{L}\gamma_i\right)$$
$$\times f(\gamma_1, \gamma_2, \ldots, \gamma_L)d\gamma_1 d\gamma_2, \ldots, d\gamma_L \tag{11}$$

where $f(\gamma_1, \gamma_2, \ldots, \gamma_L)$ denotes the joint PDF of the instantaneous SNRs. Evaluating (11) in closed form is, unfortunately, intractable, even for the case that γ_is values are statistically independent. In addition, the involved complexity increases significantly as the number of the aggregated channel bandwidths increases. Motivated by this, we attempt to derive an analytic expression for the higher-order capacity statistics over i.n.i.d $\eta-\mu$ fading channels.

A. Ergodic Capacity for i.n.i.d. Fading

For i.n.i.d $\eta-\mu$ fading channels, the PDF of γ_{end} can be expressed as [18, eq. (3)]

$$f_{\gamma_{\text{end}}}(\gamma) = \sum_{k=1}^{L}\sum_{j=1}^{\mu_k} \frac{C_{kj}}{\Gamma(j)}\gamma^{j-1}e^{-A_k\gamma}$$
$$+ \sum_{k=1}^{L}\sum_{j=1}^{\mu_k} \frac{D_{kj}}{\Gamma(j)}\gamma^{j-1}e^{-B_k\gamma} \tag{12}$$

where C_{kj} and D_{kj} are the residues of the moment-generating function $M_{\gamma_{\text{end}}}(s)$ to the poles $-A_k$ and $-B_k$, respectively, with multiplicity j. Based on this, the residues C_{kj} and D_{kj} in (12) are given by [18, eqs. (4) and (5)] as

$$C_{kj} = \frac{1}{(\mu_k - j)!} \prod_{i=1}^{L} \left(\frac{2\mu_i}{\bar{\gamma}_i} \right)^{2\mu_i} h^{\mu_i}$$
$$\times \left\{ \left[\prod_{\substack{i=1 \\ i \neq k}}^{L} \frac{1}{(s + A_i)^{\mu_i}} \right] \left[\prod_{i=1}^{L} \frac{1}{(s + B_i)^{\mu_i}} \right] \right\}^{\mu_k - j} \Bigg|_{s=-A_k}$$
(13)

$$D_{kj} = \frac{1}{(\mu_k - j)!} \prod_{i=1}^{L} \left(\frac{2\mu_i}{\bar{\gamma}_i} \right)^{2\mu_i} h^{\mu_i}$$
$$\times \left\{ \left[\prod_{i=1}^{L} \frac{1}{(s + A_i)^{\mu_i}} \right] \left[\prod_{\substack{i=1 \\ i \neq k}}^{L} \frac{1}{(s + B_i)^{\mu_i}} \right] \right\}^{\mu_k - j} \Bigg|_{s=-B_k}$$
(14)

where $A_i = 2\mu_i(h_i - H_i)/\bar{\gamma}_i$ and $B_i = 2\mu_i(h_i + H_i)/\bar{\gamma}_i$.

To this effect, the average spectral efficiency, for the specific case that μ is an arbitrary integer, can be given by [18, eq. (11)]

$$\mathbb{E}(S) = \frac{1}{\ln 2} \sum_{k=1}^{L} \sum_{j=1}^{\mu_k} \frac{C_{kj}}{\Gamma(j)} \mathcal{I}_j(A_k) + \frac{1}{\ln 2} \sum_{k=1}^{L} \sum_{j=1}^{\mu_k} \frac{D_{kj}}{\Gamma(j)} \mathcal{I}_j(B_k)$$
(15)

where

$$\mathcal{I}_n(x) = \Gamma(n) e^x \sum_{j=1}^{n} \frac{\Gamma(-n+j, x)}{x^j}$$
(16)

and $\Gamma(a, x)$ is the upper incomplete gamma function [13].

B. HOS

With the aid of (11) and by employing the PDF for an MRC in (12), one obtains

$$\mathbb{E}(S^n) = \frac{1}{\ln^n 2} \int_0^\infty \ln^n(1 + \gamma)$$
$$\times \left(\sum_{k=1}^{L} \sum_{j=1}^{\mu_k} \frac{C_{kj}}{\Gamma(j)} \gamma^{j-1} e^{-A_k \gamma} + \sum_{k=1}^{L} \sum_{j=1}^{\mu_k} \frac{D_{kj}}{\Gamma(j)} \gamma^{j-1} e^{-B_k \gamma} \right) d\gamma$$
(17)

which upon expanding (17) can be equivalently rewritten as

$$\mathbb{E}(S^n) = \frac{1}{\ln^n 2} \sum_{k=1}^{L} \sum_{j=1}^{\mu_k} \frac{C_{kj}}{\Gamma(j)} \int_0^\infty \frac{\ln^n(1 + \gamma)}{\gamma^{1-j} e^{A_k \gamma}} d\gamma$$
$$+ \frac{1}{\ln^n 2} \sum_{k=1}^{L} \sum_{j=1}^{\mu_k} \frac{D_{kj}}{\Gamma(j)} \int_0^\infty \frac{\ln^n(1 + \gamma)}{\gamma^{1-j} e^{B_k \gamma}} d\gamma. \quad (18)$$

Importantly, the aforementioned integrals can be expressed in closed form with the aid of [19, eqs. (33) and (37)]. To this end, by performing the necessary change of variables, substituting in (18), and carrying out some algebraic manipulations yields

$$\mathbb{E}(S^n) = \frac{1}{\ln^n 2} \sum_{k=1}^{L} \sum_{j=1}^{\mu_k} \frac{C_{kj}}{\Gamma(j)} \mathcal{J}_{j,n}\left(1, \frac{1}{A_k}, 1\right)$$
$$+ \frac{1}{\ln^n 2} \sum_{k=1}^{L} \sum_{j=1}^{\mu_k} \frac{D_{kj}}{\Gamma(j)} \mathcal{J}_{j,n}\left(1, \frac{1}{B_k}, 1\right) \quad (19)$$

where

$$\mathcal{J}_{j,n}\left(1, \frac{1}{A_k}, 1\right) = n! e^{A_k} \sum_{l=0}^{j-1} \frac{(-1)^{j-l-1}}{A_k^{1+l}} \binom{j-1}{l}$$
$$\times G_{n+1,n+2}^{n+2,0}\left(A_k \middle| \begin{matrix} \overbrace{1, 1, \ldots, 1}^{n+1 \ 1's} \\ \underbrace{0, 0, \ldots, 0}_{n+1 \ 0's}, 1+l \end{matrix} \right) \quad (20)$$

$$\mathcal{J}_{j,n}\left(1, \frac{1}{B_k}, 1\right) = n! e^{B_k} \sum_{l=0}^{j-1} \frac{(-1)^{j-l-1}}{B_k^{1+l}} \binom{j-1}{l}$$
$$\times G_{n+1,n+2}^{n+2,0}\left(B_k \middle| \begin{matrix} \overbrace{1, 1, \ldots, 1}^{n+1 \ 1's} \\ \underbrace{0, 0, \ldots, 0}_{n+1 \ 0's}, 1+l \end{matrix} \right) \quad (21)$$

with $G(\cdot)$ denoting the Meijer G-function [13, eq. (9.30)]. Therefore, by substituting (20) and (21) into (19), the following closed-form expression is deduced:

$$\mathbb{E}(S^n) = \sum_{k=1}^{L} \sum_{j=1}^{\mu_k} \sum_{l=0}^{j-1} \frac{(-1)^{j-l-1} C_{kj} n! e^{A_k}}{\ln^n(2) \Gamma(j) A_k^{1+l}} \binom{j-1}{l}$$
$$\times G_{n+1,n+2}^{n+2,0}\left(A_k \middle| \begin{matrix} \overbrace{1, 1, \ldots, 1}^{n+1 \ 1's} \\ \underbrace{0, 0, \ldots, 0}_{n+1 \ 0's}, 1+l \end{matrix} \right)$$
$$+ \sum_{k=1}^{L} \sum_{j=1}^{\mu_k} \sum_{l=0}^{j-1} \frac{(-1)^{j-l-1} D_{kj} n! e^{B_k}}{\ln^n(2) \Gamma(j) B_k^{1+l}} \binom{j-1}{l}$$
$$\times G_{n+1,n+2}^{n+2,0}\left(B_k \middle| \begin{matrix} \overbrace{1, 1, \ldots, 1}^{n+1 \ 1's} \\ \underbrace{0, 0, \ldots, 0}_{n+1 \ 0's}, 1+l \end{matrix} \right). \quad (22)$$

For the special case of $n = 1$, it readily follows that

$$\mathbb{E}(S) = \sum_{k=1}^{L} \sum_{j=1}^{\mu_k} \sum_{l=0}^{j-1} \frac{(-1)^{j-l-1}}{\ln(2) \Gamma(j)} \binom{j-1}{l}$$
$$\times \left[\frac{C_{kj} e^{A_k}}{A_k^{1+l}} G_{2,3}^{3,0}\left(A_k \middle| \begin{matrix} 1, 1 \\ 0, 0, 1+l \end{matrix} \right) \right.$$
$$\left. + \frac{D_{kj} e^{B_k}}{B_k^{1+l}} G_{2,3}^{3,0}\left(B_k \middle| \begin{matrix} 1, 1 \\ 0, 0, 1+l \end{matrix} \right) \right]. \quad (23)$$

It is noted here that, according to [13, eq. (9.31.1)], the Meijer G-function in (23) can be alternatively expressed as

$$G_{2,3}^{3,0}\left(A_k \left|\begin{matrix} 1,1 \\ 0,0,1 \end{matrix}\right.\right) = G_{1,2}^{2,0}\left(A_k \left|\begin{matrix} 1, \\ 0,0, \end{matrix}\right.\right) = \Gamma(0, A_k). \quad (24)$$

As a result, (23) can be also expressed as

$$\mathbb{E}(S) = \sum_{k=1}^{L} \sum_{j=1}^{\mu_k} \sum_{l=0}^{j-1} \frac{(-1)^{j-k-1}}{\ln(2)\Gamma(j)} \binom{j-1}{l}$$
$$\times \left[\frac{C_{kj}e^{A_k}}{A_k^{1+l}} \Gamma(0, A_k) + \frac{D_{kj}e^{B_k}}{B_k^{1+l}} \Gamma(0, B_k) \right] \quad (25)$$

which is a simplified algebraic representation. To this effect, by substituting the aforementioned expression into (23), one obtains the analytic expression in (15). Likewise, the second, third, and fourth moments are readily deduced yielding

$$\mathbb{E}(S^2) = \sum_{k=1}^{L} \sum_{j=1}^{\mu_k} \sum_{l=0}^{j-1} \frac{2(-1)^{j-l-1}C_{kj}e^{A_k}}{\ln^2(2)\Gamma(j)A_k^{1+l}} \binom{j-1}{l}$$
$$\times G_{3,4}^{4,0}\left(A_k \left|\begin{matrix} 1,1,1 \\ 0,0,0,1+l \end{matrix}\right.\right)$$
$$+ \sum_{k=1}^{L} \sum_{j=1}^{\mu_k} \sum_{l=0}^{j-1} \frac{2(-1)^{j-l-1}D_{kj}e^{B_k}}{\ln^2(2)\Gamma(j)B_k^{1+l}} \binom{j-1}{l}$$
$$\times G_{3,4}^{4,0}\left(B_k \left|\begin{matrix} 1,1,1 \\ 0,0,0,1+l \end{matrix}\right.\right) \quad (26)$$

$$\mathbb{E}(S^3) = \sum_{k=1}^{L} \sum_{j=1}^{\mu_k} \sum_{l=0}^{j-1} \frac{6(-1)^{j-l-1}C_{kj}e^{A_k}}{\ln^3(2)\Gamma(j)A_k^{1+l}} \binom{j-1}{l}$$
$$\times G_{4,5}^{5,0}\left(A_k \left|\begin{matrix} 1,1,1,1 \\ 0,0,0,0,1+l \end{matrix}\right.\right)$$
$$+ \sum_{k=1}^{L} \sum_{j=1}^{\mu_k} \sum_{l=0}^{j-1} \frac{6(-1)^{j-l-1}D_{kj}e^{B_k}}{\ln^3(2)\Gamma(j)B_k^{1+l}} \binom{j-1}{l}$$
$$\times G_{4,5}^{5,0}\left(B_k \left|\begin{matrix} 1,1,1,1 \\ 0,0,0,0,1+l \end{matrix}\right.\right) \quad (27)$$

$$\mathbb{E}(S^4) = \sum_{k=1}^{L} \sum_{j=1}^{\mu_k} \sum_{l=0}^{j-1} \frac{24(-1)^{j-l-1}C_{kj}e^{A_k}}{\ln^4(2)\Gamma(j)A_k^{1+l}} \binom{j-1}{l}$$
$$\times G_{5,6}^{6,0}\left(A_k \left|\begin{matrix} 1,1,1,1,1 \\ 0,0,0,0,0,1+l \end{matrix}\right.\right)$$
$$+ \sum_{k=1}^{L} \sum_{j=1}^{\mu_k} \sum_{l=0}^{j-1} \frac{24(-1)^{j-l-1}D_{kj}e^{B_k}}{\ln^4(2)\Gamma(j)B_k^{1+l}} \binom{j-1}{l}$$
$$\times G_{5,6}^{6,0}\left(B_k \left|\begin{matrix} 1,1,1,1,1 \\ 0,0,0,0,0,1+l \end{matrix}\right.\right) \quad (28)$$

respectively. In what follows, the aforementioned analytic expressions are analyzed in determining useful statistical measures.
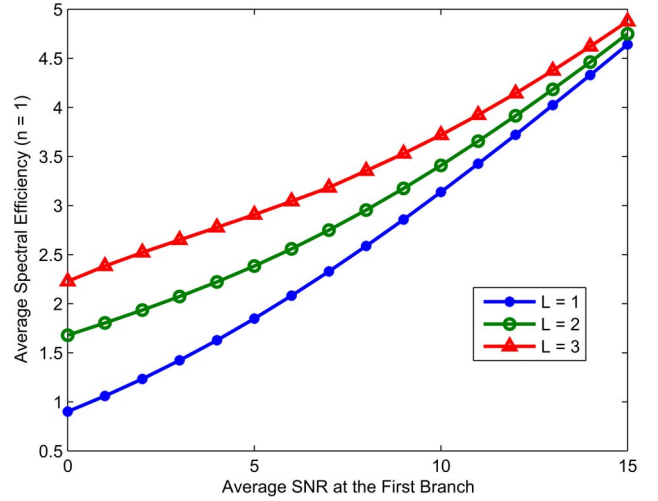

Fig. 1. Average spectral efficiency versus average SNR in the first branch for different values of L and unequal SNRs and fading parameters ($\overline{\gamma}_2 = 2$ dB, $\overline{\gamma}_3 = 4$ dB, $\mu_1 = 1.0$, $\mu_2 = 2.0$, $\mu_3 = 3.0$ and $\eta_1 = 2.3$, $\eta_2 = 1.2$, $\eta_3 = 0.4$).

C. Performance Metrics

Using (22), new analytic expressions can be straightforwardly deduced for important system's performance metrics. To this end, the first four statistical moments are derived. Based on these expressions, the following measures can be introduced as follows:

- *variance of the channel capacity* (Var)

$$\mathrm{Var} = \mathbb{E}(S^2) - (\mathbb{E}(S))^2 \quad (29)$$

- *fading figure* ($\mathcal{FF}$)

$$\mathcal{FF} = \frac{\mathbb{E}(S^2)}{(\mathbb{E}(S))^2} - 1 \quad (30)$$

- *amount of dispersion* ($\mathcal{AoD}$)

$$\mathcal{AoD} = \frac{\mathbb{E}(S^2)}{\mathbb{E}(S)} - \mathbb{E}(S) \quad (31)$$

- *skewness* ($\mathcal{S}$)

$$\mathcal{S} = \frac{\mathbb{E}(S^3) - (\mathbb{E}(S))^3}{\sqrt{\left\{\mathbb{E}(S^2)] - (\mathbb{E}(S))^2\right\}^3}} \quad (32)$$

- *kurtosis* ($\mathcal{K}$)

$$\mathcal{K} = \frac{\mathbb{E}(S^4) - (\mathbb{E}(S))^4}{\left\{\mathbb{E}(S^2) - (\mathbb{E}(S))^2\right\}^2}. \quad (33)$$

Notably, by substituting (23) and (26)–(28) into the aforementioned metrics accordingly, exact closed-form expressions are readily deduced for the performance measures mentioned previously.

IV. NUMERICAL RESULTS AND DISCUSSION

The proposed closed-form expressions are validated via Monte Carlo simulations, where an excellent match between analytical and simulation results is shown. This is performed by means of the average spectral efficiency, the fading figure, $\mathcal{AoD}$, $\mathcal{S}$, and $\mathcal{K}$ for different number of receiving paths. Specifically, Fig. 1 demonstrates the average spectral efficiency as a function of the average SNR at the first branch for the case of one, two, and three branches. The
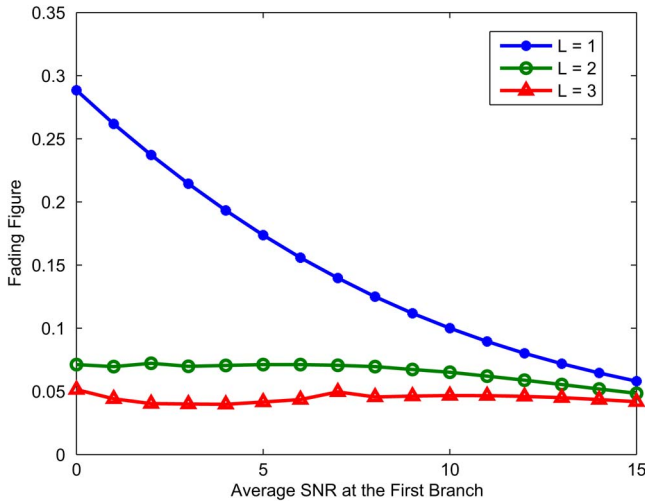
Fig. 2. Fading figure versus average SNR in the first branch for different values of L and unequal SNRs and fading parameters ($\overline{\gamma}_2 = \overline{\gamma}_3 = 1$ dB, $\mu_1 = 1.0$, $\mu_2 = 2.0$, $\mu_3 = 3.0$ and $\eta_1 = 2.3$, $\eta_2 = 1.2$, $\eta_3 = 0.4$).

Fig. 4. Skewness versus average SNR in the first branch for two different scenarios. (Scenario A: $\overline{\gamma}_2 = 2$ dB; $\mu_1 = 1$ and $\mu_2 = 2$; and $\eta_1 = 2.3$ and $\eta_2 = 1.2$. Scenario B: $\overline{\gamma}_2 = 3$ dB; $\mu_1 = 1$ and $\mu_2 = 2$; $\eta_1 = 1.2$ and $\eta_2 = 0.4$.)
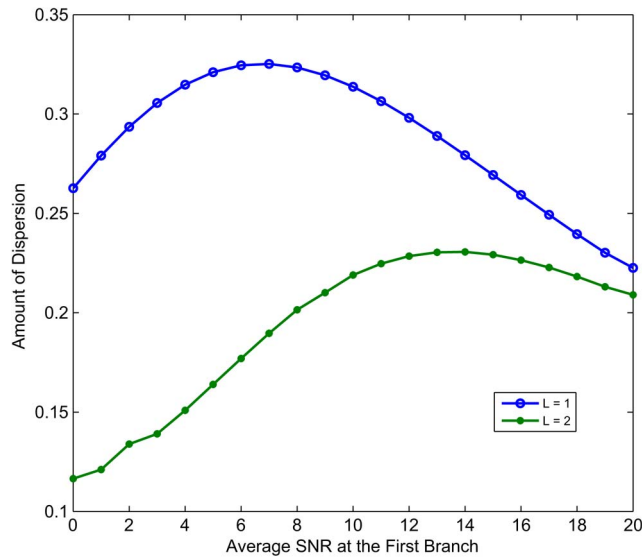

Fig. 3. Amount of dispersion versus average SNR in the first branch for different values of L and unequal SNRs and fading parameters ($\overline{\gamma}_2 = \overline{\gamma}_3 = 1$ dB, $\mu_1 = 1.0$, $\mu_2 = 2.0$, $\mu_3 = 3.0$ and $\eta_1 = 2.3$, $\eta_2 = 1.2$, $\eta_3 = 0.4$).

average SNR in the other two branches are arbitrarily selected as $\overline{\gamma}_2 = 2$ dB and $\overline{\gamma}_3 = 4$ dB, whereas the corresponding fading parameters are $\mu_1 = 1.0$, $\mu_2 = 2.0$, $\mu_3 = 3.0$ and $\eta_1 = 2.3$, $\eta_2 = 1.2$, $\eta_3 = 0.4$, respectively.[1] One can notice that the average spectral efficiency increases significantly as $\overline{\gamma}_1$ increases, while it is shown that the effect and usefulness of frequency diversity of dispersed spectrum CR is particularly critical at lower SNR values. For example, for $\overline{\gamma}_1 = 5$ dB, there is 15% difference between one and two branches and about 45% difference between one and three branches.

Figs. 2 and 3 illustrate the fading figure and the amount of dispersion as a function of the average SNR in the first branch. Regarding the former, one can observe a rapid reduction as the value of SNR and/or L increases. Indicatively, the difference between $\overline{\gamma}_1 = 2$ dB and $\overline{\gamma}_1 = 10$ dB is about 60% for $L = 1$. Likewise, for $\overline{\gamma}_1 = 1$ dB, the fading

---

[1]In addition, an exponential power decay profile can also be applied in our examples, where similar plots to the ones presented in [6] and [18] will be derived.
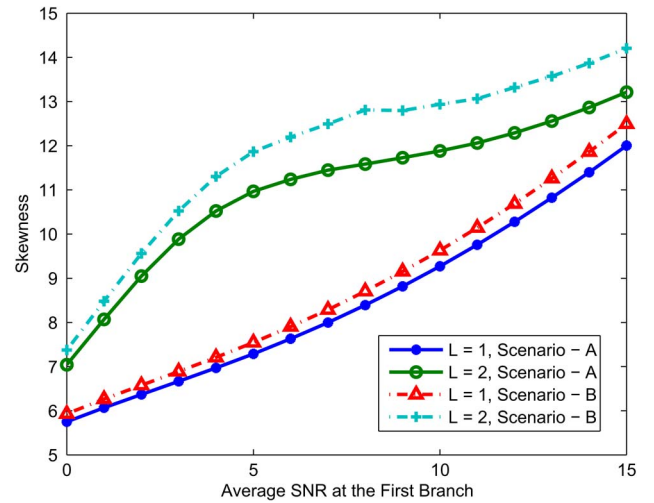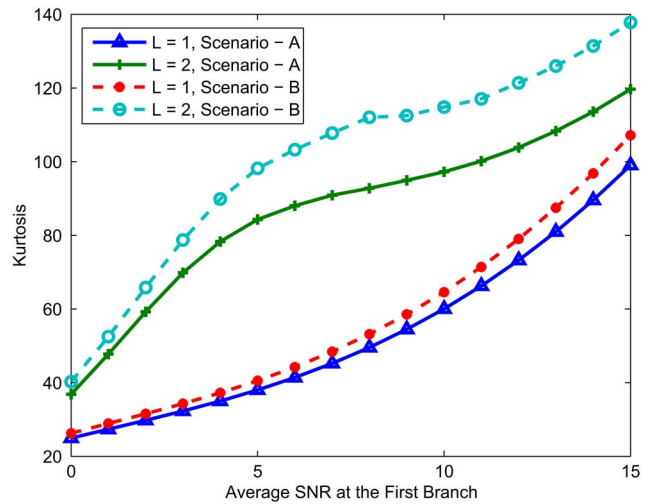

Fig. 5. Kurtosis versus average SNR in the first branch for two different scenarios. (Scenario A: $\overline{\gamma}_2 = 2$ dB; $\mu_1 = 1$ and $\mu_2 = 2$; and $\eta_1 = 2.3$ and $\eta_2 = 1.2$. Scenario B: $\overline{\gamma}_2 = 3$ dB; $\mu_1 = 1$ and $\mu_2 = 2$; $\eta_1 = 1.2$ and $\eta_2 = 0.4$.)

figure for the case of $L = 1$ is over 75% larger compared to the case of $L = 2$. The same also holds inversely for the amount of dispersion, which appears to increase for low and moderate SNR values, contrary to the high-SNR regime where it begins to decrease both for one or two antenna receivers at the UE. In addition, for $L = 1$, $\mathcal{A}o\mathcal{D}$ reaches its highest value around 5 dB, whereas for $L = 2$, the highest value of $\mathcal{A}o\mathcal{D}$ is around 13 dB. Moreover, considering the reliability percentage, i.e., $100 \times (1 - \mathcal{A}o\mathcal{D})$ [3], the data throughput is reliable when the channel capacity values do not variate significantly. Therefore, for reliable transmission of the information signals at the cognitive UE, the SNR for transmission should be selected greater than the SNR for which $\mathcal{A}o\mathcal{D}$ takes its maximum value. As expected, in both cases, the deviation between different values of L reduces at the high-SNR regime since the effect of fading becomes relatively less critical in comparison to moderate or low SNR values.

The corresponding $\mathcal{S}$ and $\mathcal{K}$ statistical measures are shown in Figs. 4 and 5, respectively, as a function of the average SNR in the first branch for unequal SNR and fading values. Specifically, two scenarios are considered for one and two branches, namely, Scenario A: $\overline{\gamma}_2 = 2$ dB; $\mu_1 = 1$ and $\mu_2 = 2$; and $\eta_1 = 2.3$ and $\eta_2 = 1.2$ and Scenario B:

$\overline{\gamma}_2 = 3$ dB; $\mu_1 = 1$ and $\mu_2 = 2$; and $\eta_1 = 1.2$ and $\eta_2 = 0.4$. One can notice the corresponding increase as the number of paths increases by one. In fact, for the considered scenario, it is shown that the increased severity of multipath fading can be compensated by increasing the number of paths. However, this appears to be particularly critical for low and moderate SNR values because, in the high-SNR regime, the effect of fading and multipath branches is, as expected, relatively reduced.

V. CONCLUSION

The present work has been devoted to the analysis of the HOS of the channel capacity of dispersed spectrum CR systems over generalized fading channels. Due to the inherent structure of the considered system, it was effectively represented as a respective MRC system. Based on this, a new analytic expression has been derived for the nth channel capacity moment, which was subsequently employed in deriving closed-form expressions for critical HOS metrics. The derived expressions were extensively validated with respective results from computer simulations, and they were utilized in analyzing the performance of the system, in terms of the average channel capacity, the fading figure, the amount of dispersion, the skewness, and the kurtosis, for unequal power and fading parameters. It has been shown that, for reliable transmission in heterogeneous bands, the SNR at the transmitter should be controlled and selected greater than the SNR for which $\mathcal{A}o\mathcal{D}$ of the channel capacity is in its higher level.

ACKNOWLEDGMENT

The statements made herein are solely the responsibility of the authors.

REFERENCES

[1] K. A. Qaraqe, H. Celebi, M. Mohammad, and A. Ekin, "Performance analysis of ad hoc dispersed spectrum cognitive radio networks over fading channels," *EURASIP J. Wir. Comm. Networking*, Springer, DOI: 10.1155/2011/849105, Jan. 2011.

[2] F. Yilmaz and M.-S. Alouini, "A unified MGF-based capacity analysis of diversity combiners over generalized fading channels," *IEEE Trans. Commun.*, vol. 60, no. 3, pp. 862–875, Mar. 2012.

[3] F. Yilmaz and M. S. Alouini, "On the computation of the higher-order statistics of the channel capacity over generalized fading channels," *IEEE Wireless Commun. Lett.*, vol 1, no. 6, pp. 573–576, Dec. 2012.

[4] F. Yilmaz, H. Tabassum, and M.-S. Alouini, "On the computation of the higher order statistics of the channel capacity for amplify-and-forward multihop transmission," *IEEE Trans. Veh. Technol.*, vol. 63, no. 1, pp. 489–494, Jan. 2014.

[5] Third-Generation Partnership Project, Sophia Antipolis Cedex, France, Rel. 10. [Online]. Available: http://www.3gpp.org/technologies/keywords-acronyms/101-carrier-aggregation-explained

[6] N. C. Sagias, F. I. Lazarakis, A. A. Alexandridis, K. P. Dangakis, and G. S. Tombras, "High order capacity statistics of diversity receivers," *Wireless Pers. Commun.*, vol. 56, no. 4, pp. 649–668, Feb. 2011.

[7] S. Gezici, H. Celebi, H. V. Poor, and H. Arslan, "Fundamental limits on time delay estimation in dispersed cognitive radio systems," *IEEE Trans. Wireless Commun.*, vol. 8, no. 1, pp. 78–83, Jan. 2009.

[8] H. Celebi, K. A. Qaraqe, and H. Arslan, "Performance analysis of TOA range accuracy adaptation for cognitive radio systems," in *Proc. 70th IEEE VTC—Fall*, Anchorage, AL, USA, Sep. 2009, pp. 1–4.

[9] M. D. Yacoub, "The $\kappa-\mu$ distribution and the $\eta-\mu$ distribution," *IEEE Antennas Propag. Mag.*, vol. 49, no. 1, pp. 68–81, Feb. 2007.

[10] P. C. Sofotasios and S. Freear, "The $\eta-\mu$/gamma composite fading model," in *Proc. IEEE ICWITS*, Honolulu, HI, USA, Aug. 2010, pp. 1–4.

[11] P. C. Sofotasios, M. Valkama, Yu. A. Brychkov, T. A. Tsiftsis, S. Freear, and G. K. Karagiannidis, "Analytic solutions to a Marcum Q-function-based integral and application in energy detection," in *Proc. CROWNCOM*, Oulu, Finland, Jun. 2014, pp. 260–265.

[12] D. B. da Costa and M. D. Yacoub, "Average channel capacity for generalized fading scenarios," *IEEE Commun. Lett.*, vol. 11, no. 12, pp. 949–951, Dec. 2007.

[13] I. S. Gradshteyn, I. M. Ryzhik, A. Jeffrey, and D. Zwillinger, *Table of Integrals, Series, and Products*, 7th ed. New York, NY, USA: Academic, 2007.

[14] P. C. Sofotasios, T. A. Tsiftsis, Yu. A. Brychkov, S. Freear, M. Valkama, and G. K. Karagiannidis, "Analytic expressions and bounds for special functions and applications in communication theory," *IEEE Trans. Inf. Theory*, vol. 60, no. 12, pp. 7798–7823, Dec. 2014.

[15] P. C. Sofotasios and S. Freear, "The $\eta-\mu$/gamma and the $\lambda-\mu$/gamma multipath/shadowing distributions," in *Proc. ATNAC*, Melbourne, VIC, Australia, Nov. 2011, pp. 1–6.

[16] N. Y. Ermolova, "Moment generating functions of the generalized $\eta-\mu$ and $\kappa-\mu$ distributions and their applications to performance evaluations of communication systems," *IEEE Commun. Lett.*, vol. 12, no. 7, pp. 502–504, Jul. 2008.

[17] N. Y. Ermolova and O. Tirkkonen, "The $\eta-\mu$ fading distribution with integer values of μ," *IEEE Trans. Wireless. Commun.*, vol. 10, no. 6, pp. 1976–1982, Jun. 2011.

[18] K. P. Peppas, "Capacity of $\eta-\mu$ fading channels under different adaptive transmission techniques," *IET Commun.*, vol. 4, no. 5, pp. 532–539, Mar. 2010.

[19] H. Shin, M. Z. Win, H. J. Lee, and M. Chiani, "On the capacity of doubly correlated MIMO channels," *IEEE Trans. Wireless Commun.*, vol. 5, no. 8, pp. 2253–2265, Aug. 2006.

Robust Transceiver Design for Two-User MIMO Interference Channel With Simultaneous Wireless Information and Power Transfer

Jian Xiao, Canhao Xu, Qi Zhang, *Member, IEEE*, Xiaobin Huang, and Jiayin Qin

Abstract—For two-user multiple-input–multiple-output interference channels with simultaneous wireless information and power transfer, we investigate robust transceiver design problem where channel uncertainties are modeled by worst case model. Our objective is to minimize worst case sum mean square error under individual transmit power constraints and worst case energy harvesting (EH) constraints. We propose to transform the quadratic EH constraints into linear matrix inequalities combined with two equality constraints. Furthermore, we propose to employ an algorithm based on constrained concave–convex procedure to alternatively optimize precoding matrices and postprocessing matrices. Simulation results demonstrate that our proposed robust transceiver design has significant performance gain over the nonrobust one.

Index Terms—Energy harvesting (EH), interference channel (IFC), multiple-input–multiple-output (MIMO), robustness, simultaneous wireless information and power transfer (SWIPT).

J. Xiao, C. Xu, Q. Zhang, and X. Huang are with the School of Information Science and Technology, Sun Yat-sen University, Guangzhou 510006, China (e-mail: xiaoj38@mail2.sysu.edu.cn; xucanhao@mail2.sysu.edu.cn; zhqi26@mail.sysu.edu.cn; huangxb2@mail2.sysu.edu.cn).

J. Qin is with the School of Information Science and Technology, Sun Yat-Sen University, Guangzhou 510006, China, and also with Xinhua College of Sun Yat-Sen University, Guangzhou 510520, China (e-mail: issqjy@mail.sysu.edu.cn).